Capture, relaxation, and recombination in two-dimensional quantum-dot superlattices

Sheng Lan,* Kouichi Akahane, Hai-Zhi Song, Yoshitaka Okada, and Mitsuo Kawabe
Institute of Applied Physics, University of Tsukuba, Tsukuba, Ibaraki 305-8573, Japan

Tetsuya Nishimura† and Osamu Wada
The Femtosecond Technology Research Association (FESTA), 5-5 Tokodai, Tsukuba 300-2635, Japan
(Received 21 July 1999; revised manuscript received 7 February 2000)

We present a systematic study of the exciton capture, relaxation, and recombination processes in two-dimensional quantum-dot superlattices (2D QDSL's) based on time-resolved photoluminescence measurements. Due to the formation of minibands in 2D QDSL's, the capture of excitons from the miniband into some large islands is found to be a quantum capture process. The capture time increases significantly with increasing excitation density. In addition, the excitons relax rapidly within the miniband. However, the relaxation becomes slower at high excitation densities. Furthermore, the fast recombination in the miniband indicates the drastic elongation of the exciton coherence length and the significant delocalization of the wave functions. Finally, the observation of radiative recombination over a wide energy region implies the relaxation of momentum conservation or the small exciton effective mass in 2D QDSL's. All phenomena suggest that the exciton dynamics in 2D QDSL's is governed by the exciton coherence length in the miniband.

I. INTRODUCTION

Stimulated by their potential applications in various electronic devices, the fabrication and characterization of quantum dots (QD's) have formed a very active research area during the last decade. The physical problems related with a single QD or an ensemble of isolated QD's have been extensively investigated.[1–3] At the same time, increasing effort has been devoted to the interaction of QD's, i.e., the coupling of two or a large number of QD's.[4–6] Up to now, ordering and coupling of QD's have received intensive studies.[7–13] The main purpose, needless to say, is to realize quantum-dot superlattices (QDSL's). Theoretically, some superior properties have been predicted for this novel system.[14–16] In experiments, high-density-ordered $In_{0.4}Ga_{0.6}As/GaAs$ QD arrays have been achieved by self-organized epitaxial growth using atomic-hydrogen-assisted molecular-beam epitaxy (H-MBE).[17,18] It has been confirmed recently by time-resolved photoluminescence (TRPL) that the extended states or minibands are formed in these QD arrays.[19,20] It means that 2D QDSL's with artificial electronic structures have been realized. Now we need to find out whether 2D QDSL's behave like quantum wells (QW's) and how the exciton dynamics will be modified as compared to conventional QD's. Obviously, the information on the capture, relaxation, and recombination in 2D QDSL's can be extracted from the analysis of the PL transients. In this paper we will present a systematic study of these processes that provides a deep understanding of 2D QDSL's. It will be shown that the exciton dynamics in 2D QDSL's is completely different from those in QW's and QD's.

II. SAMPLE AND EXPERIMENT DESCRIPTION

The 2D QDSL used in this study is the high-density-ordered $In_{0.4}Ga_{0.6}As$ QD array fabricated on a GaAs(311)B substrate by H-MBE. After growing a ~250 nm GaAs buffer layer at 580 °C, the QD's were formed at 460 °C by depositing 8.8 monolayers (ML's) $In_{0.4}Ga_{0.6}As$. The critical thickness at which the 2D-3D growth transition occurs was found to be ~6.6 ML's. Then, the QD's were covered by a ~15-nm GaAs cap layer at 400 °C. The sample fabricated at the same growth conditions but without the GaAs cap layer was used for the atomic force microscopic (AFM) characterization. The AFM image is shown in Fig. 1. The dot diameter, height, and density are estimated to be 20–30 nm, 1 nm, and $1.4 \times 10^{11}\,cm^{-2}$. It is noted that the QD's have uniform size and pack closely.

The TRPL measurements were performed by a Ti:sapphire laser with a 160-fs pulse width in combination with a streak camera, providing a time resolution of ~10 ps. The experiments were carried out at 5 K and at different excitation densities of 0.3, 1, 3, and 30 W/cm^2. The excitation energy was chosen to be 1.485 eV, which is smaller than the

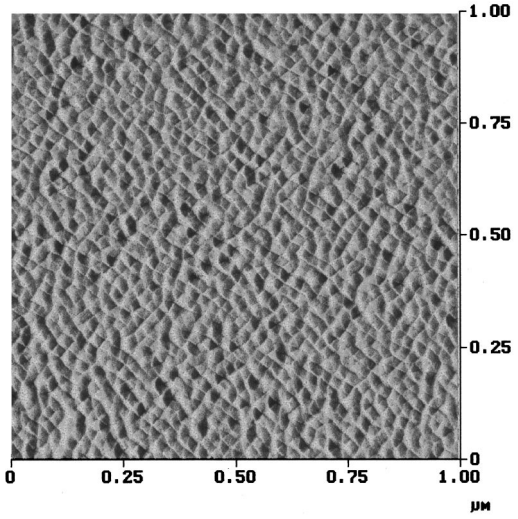

FIG. 1. AFM image of a high-density-ordered $In_{0.4}Ga_{0.6}As$ QD array fabricated on a GaAs(311)B substrate.

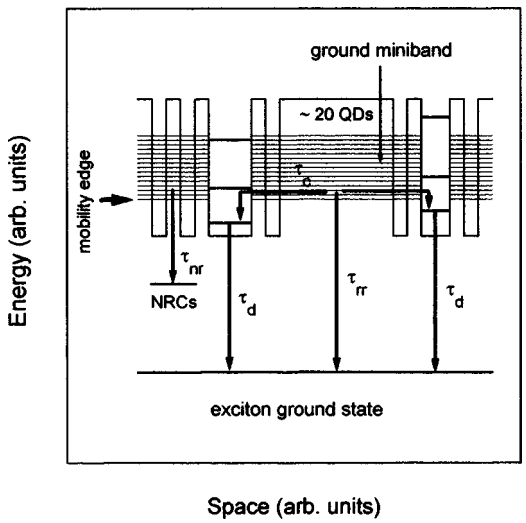

FIG. 2. Physical model describing the electronic structures of 2D QDSL's. Various decay channels are schematically illustrated. For simplicity, only the ground miniband is plotted.

GaAs barrier at 5 K (1.510 eV), in order to exclude the complicated capture process in the barrier. In measuring PL decay time as a function of photo energy, a PL spectrum is usually used as a reference.[13,21] However, the PL spectra under pulse excitation do not provide any information on rapid radiative recombination. Thus, the PL spectra under continuous-wave (cw) excitation obtained by the 514.5 nm line of an Ar^+ laser are used as references. The maximum excitation density (P_0) was set to be $\sim$4 W/cm^2 which is far below the value for the saturation of the QD's. By inserting filters with different transmission, the spectra were recorded at 4.2 K and at different excitation densities of 0.01, 0.03, 0.13, 0.25, 0.50, and $1.00P_0$.

III. PHYSICAL MODEL

In practice, we cannot avoid the formation of some large islands (large dots) originating from the coalescence of small dots. In average, approximately four large islands are found in an area of $1\times1\ \mu$m^2, giving a mean separation of $\sim$20 QD's. As can be seen later, they play important roles in determining the capture and recombination processes. Therefore, we need to treat the 2D QDSL as a disordered system containing extended states and localized states, as schematically shown in Fig. 2. The extended states or minibands originate from the strong coupling of uniform small QD's. The localized states come from the large islands that are excluded from the coupling due to much different size and energy. Although the deviation from a 2D periodic lattice can also lead to localization, we think that this kind of localization generally occurs at large islands. We will demonstrate later that the ordering in our 2D QDSL is much better than that in amorphous materials. Besides, we believe that coupling is more important than ordering in the formation of minibands because extended states or bands can be formed even in amorphous materials.

In fact, this picture is very similar to a low-density QD array. The energy levels in the low-density QD's correspond to the localized states while the subbands in the wetting layer correspond to the minibands. However, it should be emphasized that the exciton properties have been drastically changed in the minibands as compared to those in the subbands. It is also analogous to a one-dimensional (1D) superlattice (SL) in which some enlarged QW's have been intentionally introduced to detect the carrier transport in the SL.[22] The large islands thus act as natural detectors for the exciton motion in the miniband. Similarly, the ratio of the emission from the miniband to that from the large islands ($I_{\rm band}/I_{\rm island}$) can be used as a measure for the exciton coherence length in the miniband. As long as the exciton coherence length in the miniband is longer than the mean separation of two large islands, the capture of excitons from the miniband into the large islands is extremely fast. Actually, it is a quantum capture process that has been studied in multiple quantum wells (MQW's).[23] The capture time is determined by the quantum transition time between a band state and a localized state because the transport time to the large island can be neglected (Bloch wave). At low temperatures and excitation densities when the exciton coherence length is long, the capture into the large islands is faster than the radiative recombination in the miniband ($\tau_c<\tau_{rr}$). Therefore, the PL is dominated by the emission from the large islands. In order to see the emission from the miniband, we need to reduce the exciton coherence length below the mean separation of the large islands and/or saturate some large islands. Apparently, a simple and effective way to change the exciton coherence length is to increase excitation density or exciton-exciton scattering. It has been confirmed that the capture time increases rapidly with decreasing coherence length.[24] In comparison, the recombination time increases in a slower rate. As a result, some excitons will have chance to recombine in the miniband before being captured by the large islands. The emission from the miniband can be observed and will gradually dominate the PL.

Now we look at the major differences between the free excitons in the extended states and the bound excitons in the localized states. First, the free excitons have much stronger oscillator strength (or much shorter radiative lifetime) due to much longer coherence length.[16,25,26] Second, the nonradiative process (e.g., capture into deep defect centers) which can be neglected for the bound excitons is significant for the free excitons. Finally, the free excitons interact more effectively with each other and with phonons. Therefore, we can expect a sharp increase in the PL intensity and a significant broadening of the linewidth in the PL spectra with increasing excitation density if the miniband is populated. In the TRPL measurements, we should be able to see a sharp decrease of the PL decay time at the mobility edge (or the bottom of the miniband) that separates the extended states from the localized states, as generally found in conventional disordered systems.[27]

IV. TRPL MEASUREMENTS

In TRPL measurements, we trace the luminescence whose intensity is proportional to $N(t)/\tau_{rr}$, where $N(t)$ is the number of excitons in a particular energy state and τ_{rr} is the radiative lifetime. Other processes, e.g., feeding or nonradiative recombination, will influence the luminescence intensity through changing $N(t)$. For analyzing the PL transients,

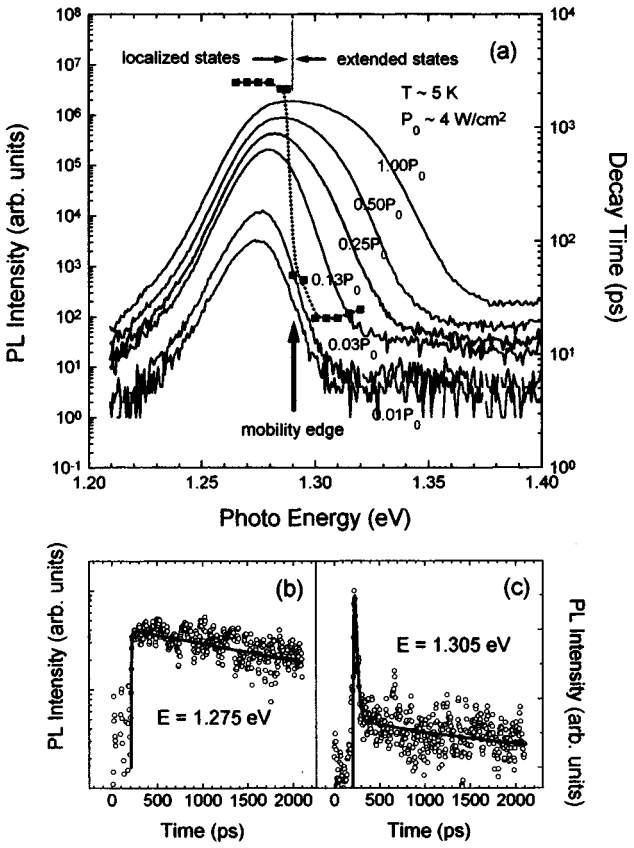

FIG. 3. (a) PL decay time as a function of photo energy measured at 1 W/cm^2 (the dotted line). The PL spectra under cw excitation are provided as references. Note that the blueshift of the peak energy and the broadening of the linewidth are accompanied with the sharp decrease of PL decay time. Typical PL transients for the localized and extended states together with the corresponding mono- and biexponential fitting results are shown in (b) and (c), respectively.

the following formula derived from a rate equation model will be used:[28]

$$I(t)\sim \exp(-t/\tau_d)-\exp(-t/\tau_r)$$

for monoexponential fitting

$$I(t)\sim[\exp(-t/\tau_{d1})-\exp(-t/\tau_r)] + \text{const}\times[\exp(-t/\tau_{d2})-\exp(-t/\tau_r)]$$

for biexponential fitting.

The physical model described in the previous section has been verified by TRPL measurements. Figure 3(a) shows the dominant PL decay time as a function of photo energy obtained at 1 W/cm^2. The excitation-dependent PL spectra under cw excitation are also provided for references. As discussed earlier, the observation of the emission from the miniband can be realized by increasing excitation density. Actually, a critical excitation density for the population of the miniband is always found. Since it depends slightly on the excitation conditions, e.g., excitation energy, laser spot size, and sample position, etc., we did not attempt to determine its accurate value by adding more measuring points. In the experiments shown in Fig. 3(a), the critical excitation density is between 0.12 and 0.52 W/cm^2 for cw excitation and is between 0.3 and 1 W/cm^2 for pulse excitation.

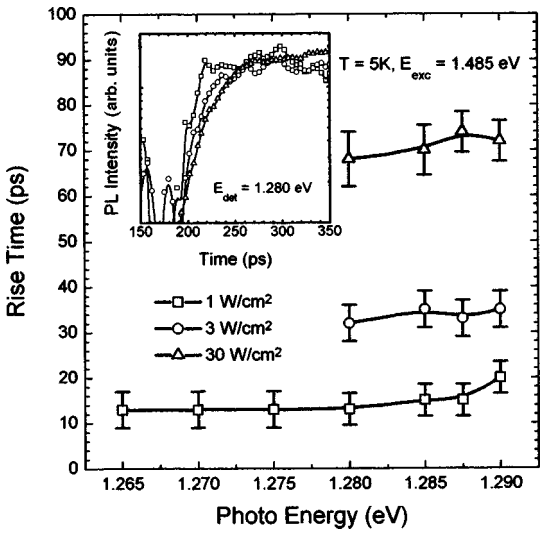

FIG. 4. PL rise time of the localized states as a function photo energy obtained at different excitation densities. A comparison at $E_{\text{det}}=1.280$ eV is presented in the inset. The error bars give the uncertainties in determining the rise times by fitting.

Below the critical value, the PL spectral shape is almost insensitive to excitation density and temperature. In addition, only a long exponential decay of 1.5–2.5 ns is observed for all detectable energy states. It indicates the localized character of the excitons and the absence of the exciton transfer. However, a clear blueshift of the peak energy as well as a significant broadening of the linewidth is observed in the PL spectra above the critical value. A sharp increase in the PL intensity is also observed.[19] Remarkably, a sharp (<1 meV) decrease of the decay time from $\sim$2.5 ns to $\sim$25 ps is found at $\sim$1.290 eV. This energy position is attributed to the mobility edge.

Since the localized states (or extended states) at different energy positions have very similar PL transients, two PL transients, which are typical for the localized states and extended states, respectively, together with mono- and biexponential fitting results are given in Figs. 3(b) and 3(c).

These experimental observations clearly justify the fact that the PL at low excitation densities is dominated by isolated large islands and the excitons begin to populate the miniband with increasing excitation density. Although it is difficult to compare exactly the exciton densities (or exciton-exciton scattering) under pulse and cw excitations, we have separately observed the population of the miniband.

A. Capture

Obviously, the capture from the miniband into the large islands should be characterized by the PL rise time of the localized states. The rise times obtained at different excitation densities are summarized in Fig. 4. A comparison at $E_{\text{det}}=1.280$ eV is shown in the inset. At 1 W/cm^2 when the exciton coherence length is long, the rise time is as short as 10–16 ps. Since it is very close to the time resolution, we think that the real capture time at lower excitation densities should be much shorter. It is consistent with the quantum capture process assumed in the model. More importantly, the

rise time is found to increase slightly to ~30 ps at 3 W/cm^2 and significantly to 60–80 ps at 30 W/cm^2. This behavior indicates that the quantum capture is alleviated with decreased coherence length by exciton-exciton scattering.[24] This excitation dependence of capture rate is opposite to that found in uncoupled QD's. There, the rise time decreases with increasing excitation density due to the accelerated capture by Auger-like processes.[29] Although the separation of two large islands is rather large (~20 QD's), the excitons captured at different positions can be immediately transferred into the large islands, justifying the coherent exciton motion in the miniband.

B. Relaxation

Before talking about the exciton relaxation in the 2D QDSL, it is helpful to discuss briefly the exciton relaxation in conventional QW's and QD's. For QW's under nonresonant excitations, excitons are generated in high-energy states. The energy relaxation is accomplished through interaction firstly with optical phonons and finally with acoustic phonons. While the former process is very fast, the latter process is rather slow. Since only the excitons at the bottom of the band can recombine radiatively (the requirement of momentum conservation),[30] the PL rise time for QW's under nonresonant excitations is very slow, typically hundred to several hundred picoseconds.[31–33] Besides, it is shortened significantly with increasing the excitation density, indicating that exciton-exciton scattering acts as an effective way to relax excess energy.[32]

In QD's, the exciton relaxation between discrete energy levels is usually not fast. Although the relaxation in some samples is as fast as several tenths picoseconds, its excitation dependence is similar to that observed in QW's. Up to now, all of the reported experiments show the same result that the PL rise time decreases with increasing excitation density,[29,34–36] implying that the Auger effect tends to accelerate the relaxation.

In our 2D QDSL, the exciton relaxation within the miniband is characterized by the PL rise time of the extended states. In Fig. 5, they are given as a function of photo energy for different excitation densities. A comparison at $E_{\mathrm{det}}=1.310$ eV is presented in the inset. In sharp contrast, the PL rise time is as short as 15–20 ps at low excitation densities. It increases gradually to 25–35 ps at 3 W/cm^2 and to 30–45 ps at 30 W/cm^2. This behavior is completely contrary to that observed in QW's and QD's. It indicates that the effect of exciton-exciton scattering on relaxation has been dramatically changed in 2D QDSL's. The relaxation within the miniband is governed mainly by the exciton coherence length in the miniband which decreases rapidly with increasing excitation density. As compared with the change in the rise time of the localized states, the change in the rise time of the extended states is relatively small. It implies that the reduction of the coherence length in the miniband has less influence on the relaxation than on the capture process. In addition, the rise times for the high-energy states are less sensitive to excitation density than those for the low-energy states near the mobility edge. It is also noted that the rise time for the miniband is slightly longer than that for the large islands. We think that the capture into the large islands from high-energy states and the fast recombination in the miniband are responsible for this abnormal behavior.

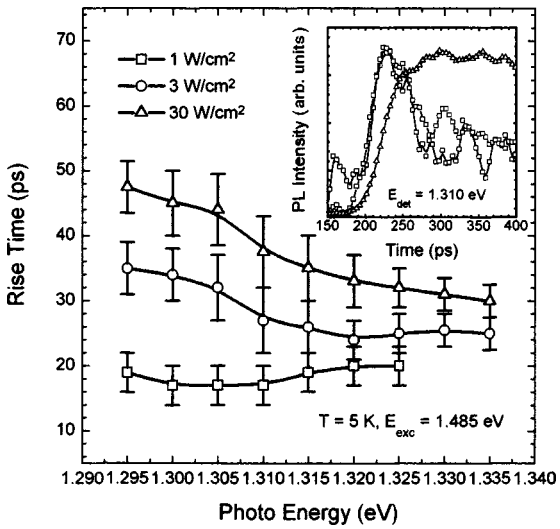

FIG. 5. PL rises time of the extended states as a function photo energy obtained at different excitation densities. A comparison at $E_{\mathrm{det}}=1.310$ eV is presented in the inset. The error bars give the uncertainties in determining the rise times by fitting.

C. Recombination

Now let us look at the exciton recombination in the miniband being a direct characterization of the exciton coherence length. The PL transients at $E_{\mathrm{det}}=1.305$ eV obtained at different excitation densities are illustrated in Fig. 6. At 1 W/cm^2, the PL transient is composed of a fast decay (τ_{d1}) of 25 ps and a slow decay (τ_{d3}) of 2.5 ns. The fast decay is

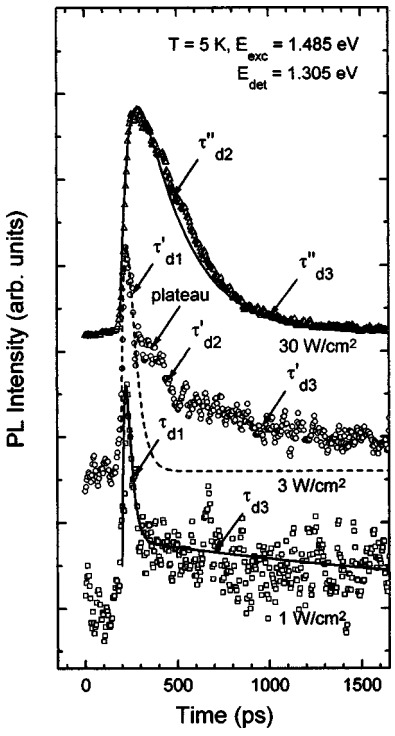

FIG. 6. PL transients at $E_{\mathrm{det}}=1.305$ eV obtained at different excitation densities.

saturated at 3 W/cm^2 in a short time and immediately at 30 W/cm^2 (cannot be resolved). Therefore, we think that the fast decay at 1 W/cm^2 contains radiative and nonradiative components that cannot be discriminated. Regardless of the character of recombination, the fast decay indicates the significant delocalization of the wave function. At 3 W/cm^2, the nonradiative centers (NRC's) are saturated in a short time after excitation. The plateau, which is shorter for high-energy states (not shown), originates from the loss of nonradiative decay channel. Naturally, the second decay (τ'_{d2}) estimated to be 50–150 ps is attributed to the radiative recombination lifetime in the miniband. So is the dominant decay (τ''_{d2}) at 30 W/cm^2, ranging from 90–270 ps. This assignment is strongly supported by the strong emission from the extended states. If the PL decay was dominated by nonradiative process as found in conventional disordered systems, e.g., II-VI ternary compounds, the emission from the extended states would be very weak.[27] In our 2D QDSL, the emission from the extended states gradually dominates the PL at high excitation densities.

Although the radiative recombination lifetimes observed at 3 and 30 W/cm^2 have been increased by exciton-exciton scattering, they are about one order of magnitude smaller than that reported in isolated QD's. Limited by the slow PL rise under nonresonant excitations, the fast decay in QW's can only be observed in resonant excitations. The radiative lifetime in 2D QDSL's observed at high excitation densities is comparable or even shorter than that reported in some high-quality QW's under resonant excitations.[33,37] Therefore, it demonstrates unambiguously the coherent exciton motion in the 2D QDSL. For incoherent exciton motion dominated by nonresonant tunneling, the exciton coherence length is still limited to the QD diameter and no significant decrease is expected for radiative recombination lifetime.[13] Besides, the PL decay time as a function of photo energy shows a rather gradual change from the long decay time region to the short decay time region, in clear distinction to the sharp transition observed in the coherent exciton motion described in our case. The slow decay (τ_{d3}, τ'_{d3}, τ''_{d3}) in all cases is attributed to the recombination in the excited states of some saturated large islands. At 30 W/cm^2, its relative intensity is very weak because most of the excitons recombine in the miniband due to decreased exciton coherence length.

One interesting and remarkable feature is that the radiative recombination can be observed in a wide energy of ~50 meV from the bottom of the miniband. We offer here two possible explanations. One explanation originates from the relief of the momentum conversation required for the allowed optical transitions because of the existence of disorder in the QD plane, similar to that in amorphous materials.[38] This consideration can also explain the similar rise times for the miniband and the large islands because the capture can occur above the band edge. However, the observation of radiative recombination from the extended states indicates a much better ordering than that in amorphous materials. The number of localized states resulting from various disorders in the 2D QDSL is even much smaller than that in II-VI ternary compounds where the PL is usually dominated by the emission from localized states.[27] Otherwise, it is impossible to see the emission from the extended states which gradually dominates the PL with increasing excitation density. Another interpretation arises from the 2D characteristics of the QDSL's. In 2D QDSL's, each QD interacts with more neighboring QD's, e.g., six nearest QD's in the closely packed case. They are expected to have wider bandwidth as compared to 1D SL's. This point is implied in some experimental results. For example, the PL peak shifts ~50 meV (to the center of the miniband) as the excitons are localized by exciton-exciton or exciton-impurity scattering or higher barrier (capped with $Al_{0.10}Ga_{0.90}As$).[19] On the other hand, the large ''lattice constant'' which is approximately equal to the QD diameter (~25 nm) leads to a much smaller first Brillouin zone. Therefore, the excitons in QDSL's are expected to have small effective mass.[18] As a result, the critical energy above which the radiative recombination is forbidden can be very large,[25,26] leading to the visible luminescence at high-energy extended states. Besides, the critical temperature above which the PL intensity begins to decay with temperature can also be very large.[26] It is responsible for the nearly constant PL up to a high temperature of ~40 K observed in the 2D QDSL (not shown). However, more rigorous experiments are needed to confirm these important properties.

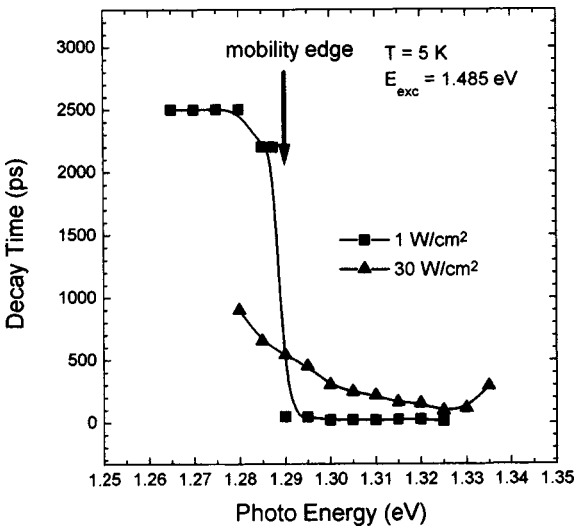

FIG. 7. Energy dependence of the PL decay time obtained at 1 and 30 W/cm^2.

The explanation given above can also interpret the observed fast PL rise time of the extended states. Because of the large critical energy for radiative recombination, the energy relaxation to the radiative recombination region can be completed by interaction only with optical phonons. The relaxation through the emission of acoustic phonons which is very slow is not necessary, leading to the fast PL rise time.

D. Mobility edge

Now we inspect the energy dependence of the dominant decay time and especially the mobility edge at 1 and 30 W/cm^2, as shown in Fig. 7. The mobility edge, which is very sharp at 1 W/cm^2, broadens significantly at 30 W/cm^2. Namely, the exciton-exciton scattering is responsible for the broadening. The increase in the decay time of the extended states is easily understood to be the reduction of coherence length. However, the mechanism for the decrease in the decay time of the localized states near to the mobility edge is relatively complicated. In general, it is ascribed to the Auger

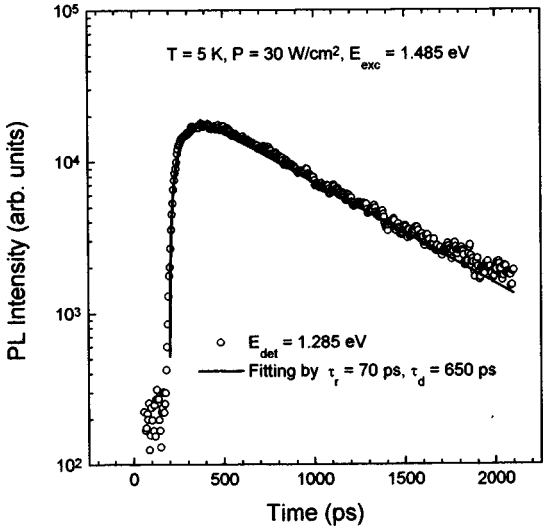

FIG. 8. PL transient at $E_{\mathrm{det}}=1.285$ eV measured at 30 W/cm^2.

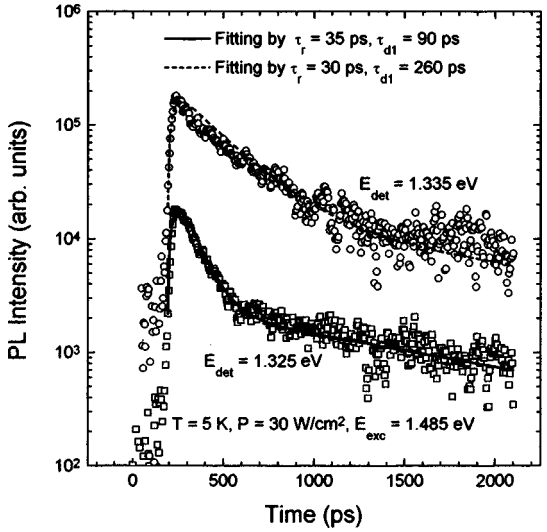

FIG. 9. A comparison of the PL transients at $E_{\mathrm{det}}=1.325$ eV and at $E_{\mathrm{det}}=1.335$ eV measured at 30 W/cm^2.

activation of the excitons into the extended states. If it was true, we should be able to see two decay processes in the PL transients because the exciton density in the extended states decays fast. After the annihilation of the excitons in the extended states, the exciton-exciton scattering is not effective and a slow decay time should be observed. However, only a single decay is observed at all time as shown in Fig. 8. Therefore, we have to consider another mechanism that is usually applied to disordered systems. Even at 30 W/cm^2, the exciton-exciton scattering is not very strong. Its main effect is to mix the extended states and localized states near the mobility edge. From another point of view, the localized states near the mobility edge are incorporated into the coupling due to the existence of exciton-exciton interaction. In order words, these localized states attain some extended feature and become partially delocalized, resulting in shorter radiative recombination lifetime.[39] As indicated by the plateau observed at 3 and 30 W/cm^2, there exists a distribution of excitons within different states. At 1 W/cm^2 when the exciton-exciton interaction is weak, the recombination lifetime is almost independent of energy. At 30 W/cm^2, when the mobility edge is broadened, the states near the mobility edge are mixture of extended and localized states. The decay time is long. At higher energy positions, the states are pure extended states, giving rise to a short decay time. However, the radiative lifetime is expected to increase with increasing wave vector. So the decay time becomes longer again at high-energy states. As can be seen in Fig. 9, the decay time at 1.335 eV is longer than that at 1.325 eV where a minimum value of ~90 ps is observed. This behavior, which is distinct from other processes, justifies the radiative nature of the decay. The strong PL intensity at the high-energy side also indicates that the decay is dominated by radiative recombination.

V. INTENSITY RATIO OF EXTENDED STATES TO LOCALIZED STATES

Now we look at the evolution of $I_{\mathrm{band}}/I_{\mathrm{island}}$ that reflects the exciton coherence in the miniband with increasing excitation density. The value of $I_{\mathrm{band}}/I_{\mathrm{island}}$ is only 1/145.2 at 0.12 W/cm^2 when the PL is dominated by the emission from the large islands. At 0.52 W/cm^2 when the excitons begin to fill the miniband, it increases drastically to 1/11.86. It becomes 1/3.51 at 1 W/cm^2 and reaches 1/1.487 at 2 W/cm^2. At 4 W/cm^2, it is larger than 1 (1.342/1) and the PL becomes dominated by the emission from the miniband. Obviously, the sharp increase in $I_{\mathrm{band}}/I_{\mathrm{island}}$ coincides exactly with the sharp increase in the PL intensity.[19] It justifies the population of the miniband in a consistent manner.

VI. CONCLUSION

In summary, the capture, relaxation, and recombination processes in 2D QDSL's have been systemically studied by TRPL measurements. It has been demonstrated that the capture from the miniband into the localized states is a quantum capture process. In addition, the relaxation within the miniband is fast. The radiative and nonradiative recombination lifetimes are found to be very short due to the drastic elongation of exciton coherence length as well as the significant delocalization of wave functions. Besides, some very important properties, e.g., relaxation of momentum conservation or small exciton effective mass, have been implied in the unique radiative characteristics of 2D QDSL's. Obviously, the novel properties that are not available in QW's and QD's make 2D QDSL's attractive for fundamental studies and promising for device applications in the near future.

ACKNOWLEDGMENTS

We acknowledge the Cryogenic Center of the University of Tsukuba for the help in PL measurements. This work was financially supported by the Ministry of Education, Science, Sports and Culture, by the Science and Technology Agency, and by the Japan Society for the Promotion of Science. A part of this work was performed in FESTA supported by New Energy and Industrial Technology Development Organization (NEDO).

*Present address: The Femtosecond Technology Research Association (FESTA), 5-5 Tokodai, Tsukuba 300-2635, Japan. Email: slan@festa.or.jp

†Present address: Advance Technology R&D Center, Mitsubishi Electric Corporation, 8-1-1 Tsukaguchi-Honmachi, Amagasaki, Hyogo 661-8661, Japan.

[1] A. Lorke, J. P. Kotthaus, and K. Ploog, Phys. Rev. Lett. **64**, 2559 (1990).

[2] D. Leonard, M. Krishnamurthy, C. M. Reaves, S. P. Denbaars, and P. M. Petroff, Appl. Phys. Lett. **63**, 3203 (1993).

[3] M. Grundmann, J. Christen, N. N. Ledentsov, J. Bohrer, and D. Bimberg, Phys. Rev. Lett. **74**, 4043 (1995).

[4] G. Schedelbeck, W. Wegscheider, M. Bichler, and G. Abstreiter, Science **278**, 1792 (1997).

[5] G. S. Solomon, J. A. Trezza, A. F. Marshall, and J. S. Harris, Jr., Phys. Rev. Lett. **76**, 952 (1996).

[6] A. F. Tsatsulnikov, A. Yu. Egorov, A. E. Zhukov, A. R. Kovsh, V. M. Ustinov, N. N. Ledentsov, M. V. Maksimov, B. V. Volovik, A. A. Suvorova, N. A. Bert, and P. S. Kopev, Semiconductors **31**, 722 (1997).

[7] G. D. Stucky and J. E. M. Dougall, Science **247**, 669 (1990).

[8] R. Notzel, J. Temmyo, and T. Tamamura, Nature (London) **369**, 131 (1994).

[9] C. B. Murray, C. R. Kagan, and M. G. Bawendi, Science **270**, 1335 (1995).

[10] G. Springholz, V. Holy, M. Pinczolits, and G. Bauer, Science **282**, 734 (1998).

[11] P. Venezuela, J. Tersoff, J. A. Floro, E. Chason, D. M. Follstaedt, Feng Liu, and M. G. Lagally, Nature (London) **397**, 678 (1999).

[12] A. Tackeuchi, Y. Nakata, S. Muto, Y. Sugiyama, T. Inata, and N. Yokoyama, Jpn. J. Appl. Phys., Part 2 **34**, L405 (1995).

[13] A. Takeuchi, Y. Nakata, S. Muto, Y. Sugiyama, T. Usuki, Y. Nishikawa, N. Yokoyama, and O. Wada, Jpn. J. Appl. Phys., Part 2 **34**, L1439 (1995).

[14] G. W. Bryant, Phys. Rev. B **40**, 1620 (1989).

[15] T. Takagahara, Solid State Commun. **78**, 279 (1991).

[16] T. Takagahara, Surf. Sci. **267**, 310 (1992).

[17] K. Akahane, T. Kawamura, K. Okino, H. Koyama, S. Lan, Y. Okada, M. Kawabe, and M. Tosa, Appl. Phys. Lett. **73**, 3411 (1998).

[18] M. Kawabe, K. Akahane, S. Lan, K. Okino, Y. Okada, and H. Koyama, Jpn. J. Appl. Phys., Part 1 **38**, 491 (1999).

[19] S. Lan, K. Akahane, K.-Y. Jang, T. Kawamura, Y. Okada, M. Kawabe, T. Nishimura, and O. Wada, Jpn. J. Appl. Phys., Part 1 **38**, 2934 (1999).

[20] S. Lan, T. Nishimura, K. Akahane, H. Z. Song, Y. Okada, O. Wada, and M. Kawabe, J. Appl. Phys. (to be published).

[21] R. Heitz, M. Veit, N. N. Ledentsov, A. Hoffmann, D. Bimberg, V. M. Ustinov, P. S. Kop'ev, and Zh. I. Alferov, Phys. Rev. B **56**, 10435 (1997).

[22] A. Chomette, B. Deveaud, A. Regreny, and G. Bastard, Phys. Rev. Lett. **57**, 1464 (1986).

[23] J. Shah, *Ultrafast Spectroscopy of Semiconductors and Semiconductor Nanostructures*, edited by M. Cardona (Springer-Verlag, Berlin, 1996), p. 318.

[24] P. W. M. Blom, C. Smit, J. E. M. Haverkort, and J. H. Wolter, Phys. Rev. B **47**, 2072 (1993).

[25] J. Feldmann, G. Peter, E. O. Gobel, P. Dawson, K. Moore, C. Foxon, and R. J. Elliott, Phys. Rev. Lett. **59**, 2337 (1987).

[26] M. Sugawara, Phys. Rev. B **51**, 10 743 (1995).

[27] S. Permogorov and A. Reznitsky, J. Lumin. **52**, 201 (1992) and references therein.

[28] F. Alder, M. Geiger, A. Bauknecht, F. Scholz, H. Schweizer, M. H. Pilkuhn, B. Ohnesorge, and A. Forchel, J. Appl. Phys. **80**, 4019 (1996).

[29] B. Ohnesorge, M. Albrecht, J. Oshinowo, A. Forchel, and Y. Arakawa, Phys. Rev. B **54**, 11532 (1996).

[30] J. Shah, *Ultrafast Spectroscopy of Semiconductors and Semiconductor Nanostructures*, edited by M. Cardona (Springer-Verlag, Berlin, 1996), Chap. 6 and references therein.

[31] J.-I. Kusano, Y. Segawa, Y. Aoyagi, S. Namba, and H. Okamoto, Phys. Rev. B **40**, 1685 (1989).

[32] T. C. Damen, J. Shah, D. Y. Oberli, D. S. Chemla, J. E. Cunningham, and J. M. Kuo, Phys. Rev. B **42**, 7434 (1990).

[33] Ph. Roussignol, C. Delalande, A. Vinattieri, L. Carraresi, and M. Colocci, Phys. Rev. B **45**, 6965 (1992).

[34] D. Oberhauser, K.-H. Pantke, W. Langbein, V. G. Lyssenko, H. Kalt, J. M. Hvam, G. Weimann, and C. F. Klingshirn, Phys. Status Solidi B **173**, 53 (1992).

[35] J. D. Berger, S. Hallstein, O. Lyngnes, W. W. Ruhle, G. Khitrova, and H. M. Gibbs, Phys. Rev. B **55**, R4910 (1997).

[36] D. Morris, N. Perret, and S. Fafard, Appl. Phys. Lett. **75**, 3593 (1999).

[37] R. Eccleston, B. F. Feuerbacher, J. Kuhl, W. W. Ruhle, and K. Ploog, Phys. Rev. B **45**, 11 043 (1992).

[38] J. Kanicki, *Amorphous & Microcrystalline Semiconductor Devices*, edited by J. Kanicki (Artech House, Boston, 1992), p. 2.

[39] C. F. Klingshirn, *Semiconductor Optics*, edited by M. Cardona (Spring-Verlag, Berlin, 1995), p. 156.